

## Observation of persistent ir hole burning in the vibrational spectrum of $\text{CN}^-$ in KBr

R. C. Spitzer, W. P. Ambrose, and A. J. Sievers

*Laboratory of Atomic and Solid State Physics and Materials Science Center, Cornell University, Ithaca, New York 14853-2501*

(Received 26 June 1986)

Both coherent and incoherent high-resolution ir techniques have been used to explore the vibrational-stretch-mode region ( $\sim 2000 \text{ cm}^{-1}$ ) of  $\text{CN}^-$  matrix isolated in KBr single crystals. At low temperatures the spectrum consists of a number of sharp lines with inhomogeneous widths  $\sim 0.05 \text{ cm}^{-1}$ . We find that most of the complexity is produced by  $\text{CN}^-$  centers which have an alkali-metal or halogen impurity ion nearby. Fourteen new centers have been identified. Some of these complex centers show persistent spectral hole production within the inhomogeneous line when the transitions are excited with a low-power ir diode laser. One extremely stable defect complex,  $\text{CN}^-:\text{Na}^+$ , has been investigated in detail both with vibrational hole burning and with fluorescence techniques. For low laser intensities and small defect densities the hole width is 50 MHz and from fluorescent decay curves the excited-state  $T_1$  time is 10 msec, the same order of magnitude found for isolated  $\text{CN}^-$  in KBr. By combining broadband Fourier transform interferometry with narrow-band diode laser hole burning, we are able to show that the persistent effect occurs when, during vibrational deexcitation, the  $\text{CN}^-$  molecule flips by  $180^\circ$  between inequivalent energy configurations generated by the presence of the nearby  $\text{Na}^+$  ion.

### I. INTRODUCTION

Spectral lines associated with the vibrational modes of matrix isolated molecules are in general not coincident with the frequencies of high-power ir-line tunable gas lasers; consequently, the high-power techniques of incoherent saturation and transient hole burning cannot be applied to identify the dominant relaxation processes in most molecular-defect-lattice combinations. With low-power tunable diode lasers, two techniques are potentially available: vibrational fluorescence, which gives the excited-state lifetime; and persistent hole burning, which identifies the excited-state dephasing time.

Solid-state vibrational fluorescence was first observed in 1972 for CO matrix isolated in van der Waals solids<sup>1</sup> and somewhat later for isomorphous  $\text{CN}^-$  in ionic crystals.<sup>2</sup> Because the radiative decay rate varies as the cube of the frequency and most vibrational modes are in the  $500\text{--}2000\text{-cm}^{-1}$  region, nonradiative processes usually dominate so the fluorescent technique is expected to have few applications in the infrared.

Persistent hole burning in optical transitions was discovered<sup>3,4</sup> in 1974 and dynamical mechanisms which produce this effect continue to be identified for an ever increasing number of solids.<sup>5-10</sup> The first measurement of persistent ir hole burning was made on 1,2-difluoroethane in rare-gas matrices<sup>11</sup> in 1979. The sources of this persistence are both the reorientation and the transformation between the *trans* and *gauche* conformations of this molecule.<sup>12</sup>

The observations of persistent spectral hole<sup>13</sup> and antihole<sup>14</sup> burning in the vibrational spectrum of  $\text{ReO}_4^-$  molecules matrix isolated in alkali halide crystals have demonstrated that persistence is possible even for a spherical-top molecule. Ultrasonic measurements<sup>15</sup> have shown that because of steric effects the two rotationally equivalent configurations for this tetrahedral molecule in

a substitutional lattice site are separated by a large energy barrier. The persistent spectroscopic changes occur when the monochromatic laser source shuffles population from one configuration to another and the return path to the ground-state configuration is blocked by the long reorientation time associated with the large energy barrier at low temperatures.

These hole-burning measurements<sup>13,16</sup> show that the hole width can be a direct measure of the homogeneous vibrational linewidth. Because of the special geometry associated with this host-molecule arrangement an important question to answer is whether or not this new technique can be used to probe the vibrational modes of other matrix isolated molecules in crystals.

This paper describes our discovery, identification, and investigation of another kind of vibrational center which shows both persistent spectral effects and vibrational fluorescence at low temperatures.<sup>17</sup> The center is the  $\text{CN}^-$  molecule with a near-neighbor  $\text{Na}^+$  impurity ion in place of one of the host  $\text{K}^+$  ions in KBr. The hole-burning process is spectrally very different from that observed for the spherical-top molecule; for this new center the oscillator strength is transferred outside of the inhomogeneous linewidth during burning while for the previous infrared system the oscillator strength is transferred by only a few homogeneous widths. By combining diode laser spectral burning together with a fast Fourier transform broad-band spectroscopic probe beam, it has been possible to locate and study the polarization properties of the frequency shifted antihole. The data demonstrate that the two inequivalent ground-state configurations of the vibrational center correspond to either the carbon or the nitrogen of the  $\text{CN}^-$  molecule being nearest to the  $\text{Na}^+$  impurity ion.

In Sec. II the samples are identified and the diode laser and high-resolution interferometer techniques reviewed. The spectroscopy, hole-burning properties, and stability of

TABLE I. KCN-doped KBr sample information.

Boule no.	CN <sup>-</sup> concentration in the crystal (mol %)	Other dopants in the melt (mol %)	Na <sup>+</sup> :CN <sup>-</sup> concentration in the crystal (mol %)
61285	0.006		$1.2 \times 10^{-4}$
701055	0.01		$2.2 \times 10^{-4}$
7002194 <i>W</i>	0.01		
701035	0.05		$8.0 \times 10^{-4}$
702163	0.29		$4.0 \times 10^{-3}$
8405044 <i>W</i>	0.5 <sup>12</sup> C <sup>14</sup> N		
8503016 <i>W</i>	0.015	0.4 NaBr	$9.5 \times 10^{-4}$
8410104 <i>W</i>	0.12	0.2 LiBr	
8410264 <i>W</i>	0.12	0.2 NaBr	$1.5 \times 10^{-2}$
8411144 <i>W</i>	0.13	0.2 RbBr	
8411134 <i>W</i>	0.13	0.2 KCl	

the CN<sup>-</sup> complex centers are described in Sec. III. In addition the most stable hole-burning center, the CN<sup>-</sup>:Na<sup>+</sup> complex is identified and shown to exhibit vibrational fluorescence. Section IV describes those hole-burning experiments which enable the dynamics of the persistent effect in CN<sup>-</sup>:Na<sup>+</sup> to be identified. The center behaves as a two-level system with a barrier of 1500 K separating the two configurations.

## II. EXPERIMENTAL DETAILS

The doped alkali halide samples were grown by the Czochralski method at Cornell Materials Science Center. A complete list of the KBr crystals is compiled in Table I. Note that some of the samples have been double doped in order to reproduce the spectroscopic features observed in nominally pure KBr doped with CN<sup>-</sup>. The actual mol % concentration,  $C$ , of CN<sup>-</sup> listed in Table I has been established by comparing the measured low-temperature line strength,  $S$  (cm<sup>-2</sup>), with the vibrational mode oscillator strength,<sup>2</sup>  $f = 0.03$ . The appropriate relation connecting these quantities is

$$C = (2.29 \times 10^{-3}) S \text{ mol \%} . \quad (1)$$

High-concentration samples can be calibrated at room temperature by measuring the absorption coefficient,  $\alpha$ , of the broad absorption band at a fixed frequency. For the KBr host with  $\alpha$  evaluated at 2086 cm<sup>-1</sup> the appropriate relation is

$$C = (1.61 \times 10^{-1}) \alpha \text{ mol \%} . \quad (2)$$

All broad-band spectroscopic data have been obtained with a commercial Fourier transform infrared interferometer (FTIR) operating at a resolution of 0.04 cm<sup>-1</sup>. For this high-resolution study the samples are cooled to 1.7 K with a variable temperature optical cryostat which contains cooled ZnSe and room-temperature NaCl windows. A CO gas cell at 10-mTorr pressure is used to check the frequency calibration of the FTIR.

Hole-burning measurements have been carried out in the 5- $\mu$ m region with a GM or a Laser Analytics semicon-

ductor diode laser (SDL). These lasers are housed in a laser analytics variable temperature cold head and have a frequency jitter of about 10 MHz which is much less than the widths of the persistent holes studied here. The SDL's can be scanned continuously over a frequency interval of a fraction of 1 cm<sup>-1</sup> without a mode hop. A 2.54 cm long Ge etalon is used to estimate hole linewidths. The SDL's are operated cw in multimode at powers between 60 and 700 mW to burn persistent holes. The single-mode intensities on the sample are between 1 mW/cm<sup>2</sup> and 1.5 W/cm<sup>2</sup>. Neutral density filters are inserted in front of the sample to reduce the intensity by as much as 10<sup>4</sup> so that the hole spectral shapes can be measured without inducing persistent changes.

The experimental arrangement for hole burning is shown in Fig. 1. The ZnSe Brewster angle polarizer in combination with a 5.3- $\mu$ m CdS  $\frac{1}{2}$  wave plate is used to produce linearly polarized light at any orientation with respect to the cleaved crystal (100) axis. After the cryostat the beam passes through a  $\frac{3}{4}$  meter monochromator so that the additional unwanted longitudinal diode modes can be rejected. The transmitted signal is detected with a

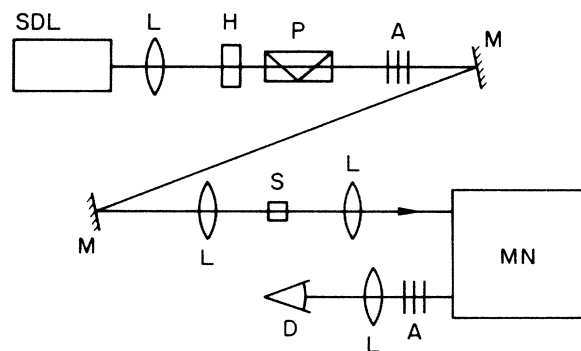


FIG. 1. Experimental arrangement for hole-burning measurements. *A*, neutral density filter attenuators; *D*, InSb detector; *H*, CdS 5.3- $\mu$ m  $\frac{1}{2}$ - $\lambda$  plate; *L*, BaF<sub>2</sub> lenses; *S*, sample; *M*, mirrors; *MN*,  $\frac{3}{4}$ -m monochromator; *P*, ZnSe Brewster angle polarizer; *SDL*, semiconductor diode laser.

77-K InSb photovoltaic detector and the spectra are averaged with a digital storage oscilloscope. The absolute frequency of each SDL mode is obtained from the CO<sub>2</sub> laser calibrated monochromator used for mode separation.

For the vibrational fluorescence experiments samples are irradiated at 2078.7 cm<sup>-1</sup> with 300-μJ, 100-nsec pulses produced by doubling a CO<sub>2</sub> TEA laser pump with a Te crystal. The sample is located in the same variable temperature crystal used for the hole-burning experiments. Radiation emitted by the sample at 90° to the pump beam direction is imaged onto the monochromator and measured with the InSb photodetector. At a given grating setting the time-resolved fluorescence decay signal is recorded from the digital storage oscilloscope. The data is also numerically integrated to give the total energy.

Incoherent saturation measurements have been made by monitoring the sample transmission versus incident laser intensity. The intensity at the sample is varied by moving the neutral density filters one by one from one side of the cryostat to the other so that errors associated with non-linear InSb detector response are minimized. After each measurement the diode laser is scanned through the saturation frequency to ensure that any persistent spectral holes which had been inadvertently burned are less than 2% deep.

In one series of experiments the high brightness and monochromatic property of the SDL is used in conjunction with the low intensity but broad-bandwidth measuring capability of the FTIR spectrometer to identify the frequency shifted product states. Since even at the highest resolution the FTIR cannot resolve a burned hole, the SDL is swept in frequency over the entire inhomogeneous width to erase as much of this absorption line as possible. An FTIR spectrum is taken and then the sample temperature is raised above the hole erasure temperature for 5 min. Upon cooling to 1.7 K a reference FTIR is taken. The difference between these spectra gives the diode-induced change over a large frequency interval.

### III. PERSISTENT HOLE-BURNING CENTERS IN CN<sup>-</sup>-DOPED KBr

#### A. Discovery

##### 1. Spectroscopy

The spectral features for CN<sup>-</sup>-doped alkali halide crystals have been measured by a number of investigators.<sup>18-21</sup> Early studies<sup>18</sup> showed that at low temperatures the CN<sup>-</sup> molecule reorients by tunneling motion while later work<sup>20</sup> demonstrated that the equilibrium orientations of the molecule are along the equivalent [111] axes in the face-centered-cubic lattice. In the most recent spectroscopic work which was carried out at a resolution of 0.1 cm<sup>-1</sup>, it was claimed<sup>21</sup> that the tunneling structure for KCl, KBr, and KI has been resolved. With increasing lattice constant of the host the stretch-mode absorption appeared to shift from two satellite peaks into a central line. Since the relative strengths of the two satellites and the central component were found to vary from sample to sample the satellites have been assigned to tunneling

centers and the central line to localized ones. Because KBr:CN<sup>-</sup> was reported<sup>21</sup> to have both satellite and central components of about the same strength indicating equal concentrations of tunneling and localized centers, our search for persistent effects has been made in this lattice-defect system.

Figure 2(a) shows the absorption coefficient in the stretch-mode frequency region of a KBr crystal doped with 0.05 mol% KCN. The vertical dashed line in the figure divides the results up into two frequency regions. The absorption lines for frequencies larger than 2100 cm<sup>-1</sup> are associated with different isotopes of the NCO<sup>-</sup> molecule, a common impurity in the KCN dopant. The frequencies of these modes are recorded in Table II. From diode laser measurements these lines have inhomogeneous widths of about 0.05 cm<sup>-1</sup> at liquid-helium temperatures. Since these absorption lines do not show persistent hole burning this center will not be considered in the remainder of the paper. The absorption lines at frequencies below 2100 cm<sup>-1</sup> are associated with the CN<sup>-</sup> stretch vibration. The center frequencies and line identifications are also given in Table II.

The fine structure near the (<sup>12</sup>C<sup>14</sup>N<sup>-</sup>) absorption line of a KBr + 0.01 mol% KCN crystal can be seen more

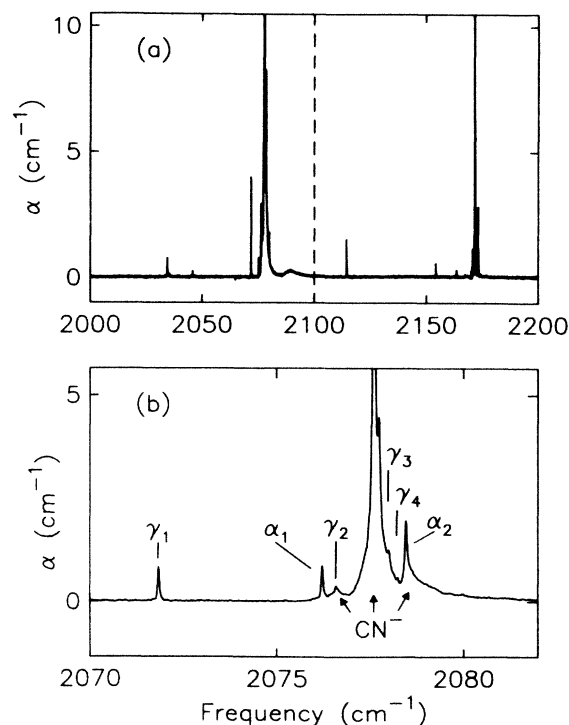


FIG. 2. Absorption spectra of CN<sup>-</sup>-doped KBr. (a) Impurity-induced absorption coefficient in the CN<sup>-</sup> stretch-mode region for a KBr + 0.05 mol% KCN sample. The vertical dashed line divides the spectrum into two parts: on the right, isotope lines of NCO<sup>-</sup>; on the left, lines of CN<sup>-</sup>. The center frequencies are recorded in Table II. (b) Enlargement of the CN<sup>-</sup> region for a KBr + 0.01 mol% KCN sample. Persistent hole burning has been observed on the lines labeled α<sub>1</sub>, α<sub>2</sub>, γ<sub>1</sub>, γ<sub>2</sub>, γ<sub>3</sub>, and γ<sub>4</sub>. The sample temperature is 1.7 K and the FTIR instrumental resolution is 0.04 cm<sup>-1</sup>.

TABLE II. Center frequencies and hole-burning properties of the different vibrational modes in the KBr:CN<sup>-</sup> spectrum at 1.7 K.

Vibrational center	Frequency (cm <sup>-1</sup> )	Hole burns?
<sup>14</sup> N <sup>12</sup> C <sup>16</sup> O <sup>-</sup>	2171.57	no
<sup>14</sup> N <sup>12</sup> C <sup>18</sup> O <sup>-</sup>	2163.45	no
<sup>15</sup> N <sup>12</sup> C <sup>16</sup> O <sup>-</sup>	2154.23	no
<sup>14</sup> N <sup>13</sup> C <sup>16</sup> O <sup>-</sup>	2114.43	no
<sup>10</sup> B <sup>16</sup> O <sub>2</sub> <sup>-</sup>	2030.96	
<sup>11</sup> B <sup>16</sup> O <sub>2</sub> <sup>-</sup>	1960.71	
<sup>12</sup> C <sup>14</sup> N <sup>-</sup>	2077.60	no
<sup>12</sup> C <sup>15</sup> N <sup>-</sup>	2045.80	no
<sup>13</sup> C <sup>14</sup> N <sup>-</sup>	2034.46	no
<sup>12</sup> C <sup>14</sup> N <sup>-</sup> :Na <sup>+</sup>		
( $\gamma_1$ )	2071.83	yes
( $\gamma'_1$ )	2077.75	yes
( $\gamma_2$ )	2076.59	yes
( $\gamma_3$ )	2077.99	yes
( $\gamma_4$ )	2078.22	yes
<sup>12</sup> C <sup>15</sup> N <sup>-</sup> :Na <sup>+</sup> ( $\gamma_1$ )	2040.22	
<sup>13</sup> C <sup>14</sup> N <sup>-</sup> :Na <sup>+</sup> ( $\gamma_1$ )	2028.79	
<sup>12</sup> C <sup>14</sup> N <sup>-</sup> :Cl <sup>-</sup>		
( $\alpha_1$ )	1076.21	yes
( $\alpha_2$ )	2078.45	yes
<sup>12</sup> C <sup>14</sup> N <sup>-</sup> :Li <sup>+</sup>		
( $\beta_1$ )	2066.81	no
( $\gamma_1$ )	2074.07	no
( $\beta_2$ )	2078.14	no
( $\beta_3$ )	2078.39	no
( $\gamma'_1$ )	2083.57	no
( $\beta'_1$ )	2084.43	no
<sup>12</sup> C <sup>14</sup> N <sup>-</sup> :Rb <sup>+</sup> ( $\gamma_2$ )	2076.84	no
<sup>12</sup> C <sup>14</sup> N <sup>-</sup> : <sup>12</sup> C <sup>14</sup> N <sup>-</sup>	2079.98	no
<sup>12</sup> C <sup>14</sup> N <sup>-</sup> : <sup>12</sup> C <sup>14</sup> N <sup>-</sup>	2075.22	no

clearly in Fig. 2(b). At 1.7 K the spectrum is characterized by one strong central line with a large line width (FWHM of 0.1 cm<sup>-1</sup>) surrounded by lines which have much narrower linewidths (FWHM of 0.04 cm<sup>-1</sup>) and are labeled  $\alpha_1$ ,  $\alpha_2$ ,  $\gamma_1$ ,  $\gamma_2$ ,  $\gamma_3$ , and  $\gamma_4$  in the figure. By 50 K all complex lines except  $\gamma_1$  have disappeared. A particular greek letter is used to specify the absorption line produced by the CN<sup>-</sup> plus nearby impurity ion. The numerical subscript is to indicate whether the impurity ion is in the first allowed shell for that ionic charge or more distant from the molecule.

The three components associated with isolated CN<sup>-</sup> by Beyer<sup>21</sup> are identified by the arrows in Fig. 2(b). This spectrum with one strong central component is somewhat different from the three components of equal strength

shown in Fig. 18 of Ref. 21. To see if this difference is associated with the concentration difference between the two crystals we examined a second crystal grown with lower CN<sup>-</sup> concentration, namely, 0.006 mol %. The relative heights of the various features in the 1.7-K spectrum of this sample, at 0.04-cm<sup>-1</sup> resolution, are identical to that shown in Fig. 2(b). The hole-burning measurements which are described below lead us to conclude that the central line and related broad structure can be attributed to the isolated CN<sup>-</sup> ion and the nearby sharp lines to CN<sup>-</sup> ion impurity complexes.

## 2. Hole burning

No hole burning is observed in the central line in Fig. 2(b). The sharp spectral lines labeled  $\alpha_1$ ,  $\alpha_2$ ,  $\gamma_1$ ,  $\gamma_2$ ,  $\gamma_3$ , and  $\gamma_4$  show persistent changes when probed with a diode laser. When the holes are burned and then probed as a function of frequency with a low intensity beam, the resultant signature is very different from that observed for the ReO<sub>4</sub><sup>-</sup> molecule. For each of the absorption lines  $\alpha_1$ ,  $\alpha_2$ ,  $\gamma_1$ ,  $\gamma_2$ ,  $\gamma_3$ , and  $\gamma_4$  the oscillator strength removed from the laser frequency does not reappear at another frequency within the inhomogeneous width whereas in the ReO<sub>4</sub><sup>-</sup> case the oscillator strength did remain within the inhomogeneous width.

Examples of hole burning in the three absorption lines  $\alpha_1$ ,  $\alpha_2$ , and  $\gamma_1$  are shown in Fig. 3. The hole burned in the  $\alpha_1$  line which is shown in Fig. 3(a) can be made 100% deep but washes out after about 3 min in the dark. Similar behavior is seen for the  $\gamma_2$ ,  $\gamma_3$ , and  $\gamma_4$  lines. The hole burned in the  $\alpha_2$  line [Fig. 3(b)] is quite shallow and disappears about 30 sec after the laser is turned off. The hole burned in the  $\gamma_1$  absorption line can also be made 100% deep and has the interesting property that it appears to be permanent as long as the sample is maintained at liquid-helium temperatures. Figure 3(c) shows the spectrum before and after two holes have been burned in the  $\gamma_1$  line. Note that in all three spectra no evidence of the corresponding antiholes can be seen.

Since the laser only excites those defects which are within a homogeneous linewidth of the laser frequency, the production and investigation of a resulting hole can, in principle, provide information on the homogeneous line shape and dephasing time,  $T_2$ , in the excited state. To obtain intrinsic information shallow holes must be burned at small laser intensities so that saturation effects are negligible.<sup>22</sup> At high laser intensity stimulated emission will cause a decrease in the excited-state lifetime and power broadening of the homogeneous linewidth results. An incoherent saturation measurement on the  $\gamma_1$  absorption line gives a saturation intensity,  $I_s$ , between 5 and 15 mW/cm<sup>2</sup>. Figure 4 shows the persistent hole burned in the  $\gamma_1$  mode at three different laser intensities, namely, 1, 10, and 100 mW/cm<sup>2</sup>. The results demonstrate that the broadening is coming from the saturation behavior of the two-level system. At lower laser intensities, shallow hole widths of 50, 70, and 73 MHz have been measured for defect concentrations of  $2.2 \times 10^{-4}$  mol %,  $8 \times 10^{-4}$  % and  $9.5 \times 10^{-4}$  %, respectively, in the  $\gamma_1$  line indicating that a weak concentration dependence of the homogeneous

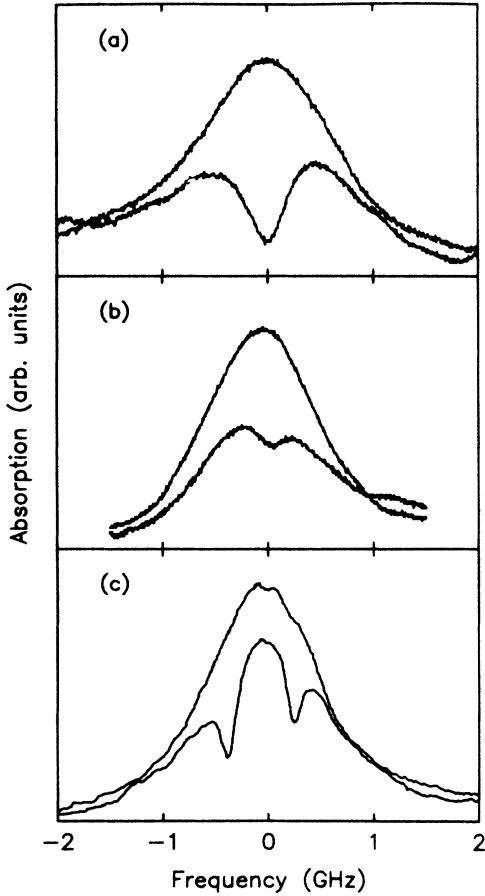


FIG. 3. Examples of persistent hole-burning spectra. Both before burning and after is shown for each case: (a)  $\alpha_1$  mode, (b)  $\alpha_2$  mode, and (c)  $\gamma_1$  mode. All the holes are power broadened. The sample temperature is 1.7 K.

linewidth occurs. One sample with a  $\gamma_1$  defect concentration of  $4.0 \times 10^{-3}$  mol % is observed to have a hole width of 500 MHz which is much larger than expected from a linear extrapolation of the lower concentration data. A different dephasing mechanism must be active for this larger defect density.

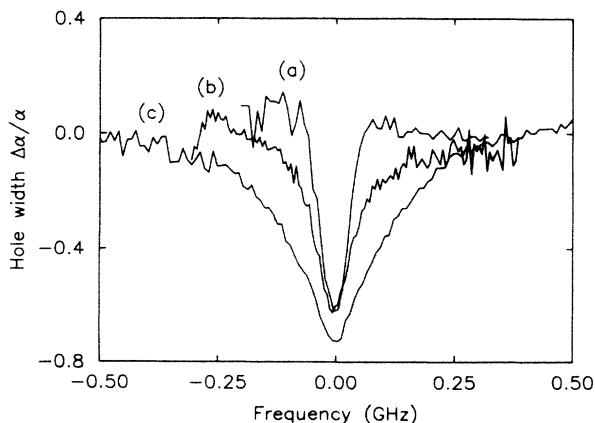


FIG. 4. Power broadening of persistent holes in the  $\gamma_1$  mode spectrum. Burn intensity at the sample is (a) 1 mW/cm<sup>2</sup>, (b) 10 mW/cm<sup>2</sup>, (c) 100 mW/cm<sup>2</sup>.

### 3. Stability

The stability of the holes burned in the  $\gamma_1$  absorption line has been determined by monitoring the spectrum with a probe beam while the sample temperature is varied. Figure 5 shows a number of scans at different temperatures: Trace (a) shows the spectrum with two holes at 1.7 K, trace (b) the same sample at 15 K, trace (c), at 25 K and trace (d), at 35 K. At this temperature the spectrum looks nearly featureless yet when the sample is cooled back down to 1.7 K, trace (e), the original spectrum is covered. To erase these holes in a reasonable amount of time the sample temperature must be increased to at least 48 K.

Figure 6 shows another unusual property of hole burning in the  $\gamma_1$  absorption line. By sweeping the diode laser frequency over a fixed interval for about 2 min at an intensity of 500 mW/cm<sup>2</sup>, a slot can be milled in the absorption line [Fig. 6(a)]. If the sweeping interval is increased to include the entire absorption line then the inhomogeneous line is erased [Fig. 6(b)] after 80 min. These unusual experimental properties led us to focus our investigation on the  $\gamma_1$  line in order to identify the nature of the lattice defect which produces such stable holes at low temperature with this unusual memory pattern.

### B. CN<sup>-</sup>:Na<sup>+</sup> complex

A systematic investigation of the influence of different cation and anion dopants on the CN<sup>-</sup> vibration spectrum has led us to the correct identification of the  $\alpha_1$ ,  $\alpha_2$ ,  $\gamma_1$ ,  $\gamma_2$ ,  $\gamma_3$ , and  $\gamma_4$  absorption lines labeled in Fig. 2. Figure 7 shows the influence of different alkali impurity ions on

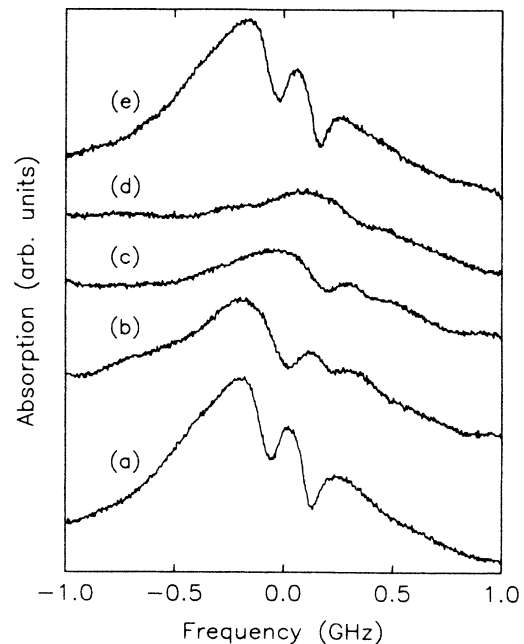


FIG. 5. Stability of the persistent hole in the  $\gamma_1$  mode. The temperature is cycled from 1.7 to 35 K and back. The sample temperatures in the four cases shown are (a)=1.7, (b)=15, (c)=25, (d)=35, and (e) back to 1.7 K again.

the  $\text{KBr}:\text{CN}^-$  vibrational spectrum. The absorption spectrum for  $\text{KBr} + 0.12 \text{ mol } \% \text{ KCN} + 0.2 \text{ mol } \% \text{ NaBr}$  [Fig. 7(a)] shows that the  $\gamma_1$ ,  $\gamma_2$ ,  $\gamma_3$ , and  $\gamma_4$  modes have increased strength over that shown in Fig. 2 for a crystal which did not have intentional  $\text{Na}^+$  doping. In addition the strength of the  $\gamma_1$  mode is found to vary linearly with the amount of  $\text{NaBr}$  added to the melt.

Figure 7(b) shows that the perturbation produced by double doping with 0.2 mol %  $\text{LiBr}$  causes six new lines to appear. These frequencies for 1.7 K are tabulated in Table II. The lines are present at all temperatures. A strong concentration gradient along the boule length has enabled us to make concentration-dependent measurements. A linear  $\text{Li}^+$  dependence is found for the  $\gamma$  lines and a quadratic dependence for the  $\beta$  lines identified in Fig. 7(b). From an earlier study<sup>23</sup> it has been shown that the  $\text{Li}^+$  impurity in  $\text{KBr}$  readily forms paraelectric pairs and it may be that a similar clustering behavior is nucleated by the  $\text{CN}^-$  molecule in this case. Since hole burning has not been observed for this alkali dopant the labeling in Fig. 7(b) is different from Fig. 7(a). The oscillator strength of each transition has been measured as a function of temperature and when the sum of the strengths of two lines is observed to be temperature independent they are given the same label. The prime is to indicate which of the two lines increases in strength with increasing temperature. This notation is used to indicate that the mechanism behind this sharp line spectrum is probably the same as for the  $\text{Na}^+$  case although without the persistent signature the identification is not complete.

Finally double doping with 0.2 mol %  $\text{RbBr}$  produces a

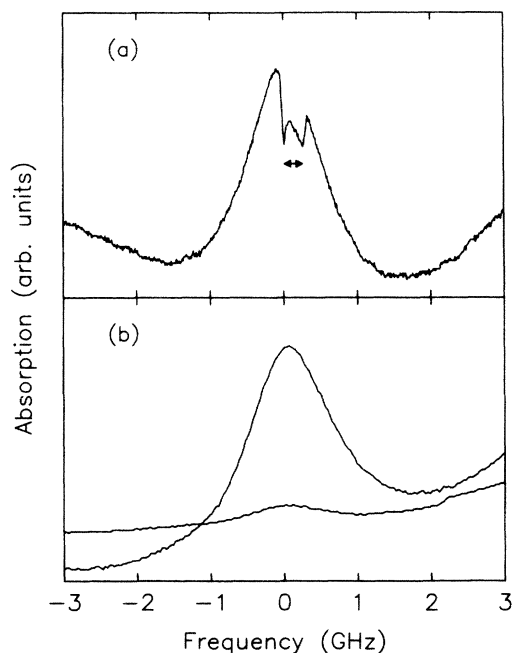


FIG. 6. Milling and erasing the  $\gamma_1$  mode. (a) Sweeping the diode frequency over a fixed frequency interval (arrow width) mills a slot in the absorption line. (b) Sweeping the diode frequency over  $\pm 2 \text{ GHz}$  for 80 min erases the  $\gamma_1$  line. Sample temperature is 1.7 K.

single new line,  $\gamma_2$ , close to the main  $\text{CN}^-$  stretch-mode vibration frequency. It disappears by 25 K. The spectral lines identified in this double doping study demonstrate that the vibrational center which produces the  $\gamma_1$  mode in Fig. 7(a) is a  $\text{CN}^-:\text{Na}^+$  complex.

### C. Fluorescence

Yang and Lüty discovered that excited  $F$  centers in alkali halides can transfer some energy to nearby  $\text{CN}^-$  ions which in turn fluoresce in the  $5\text{-}\mu\text{m}$  wavelength region.<sup>2,24</sup> Subsequent direct vibrational excitation studies of the fluorescence from isolated  $\text{CN}^-$  ions at low temperatures by Tkach *et al.*<sup>25,26</sup> have shown the importance of an efficient vibrational energy exchange process when the  $\text{CN}^-$  concentration exceeded 0.01 mol %. Manipulation of this transfer process has led to the development of the first solid-state vibrational laser.<sup>25,27,28</sup> Here we use this same vibrational energy exchange process to examine the excited-state lifetime of the  $\text{CN}^-:\text{Na}^+$  center.

Roughly  $300\text{-}\mu\text{J}$ , 100-nsec pulses produced by the second-harmonic generation from a  $\text{CO}_2$  TEA laser have been used to pump the  $\text{KBr}:\text{CN}^-$  vibrational fundamental at  $2078.7 \text{ cm}^{-1}$ . For low- $\text{CN}^-$  concentration at 1.7 K the time-resolved fluorescence signal from the fundamental

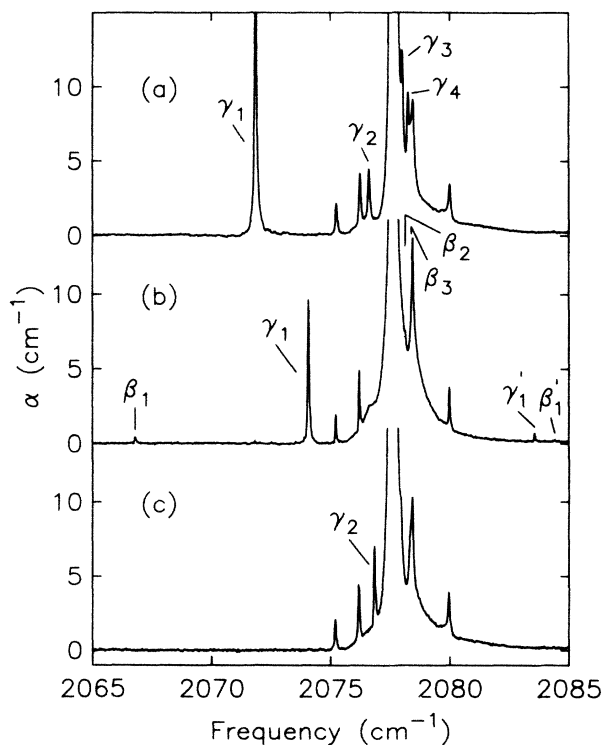
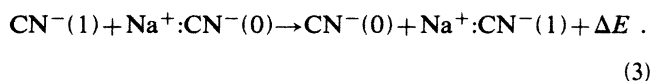


FIG. 7. Influence of alkali ion impurities on  $\text{CN}^-$  vibrational spectrum in  $\text{KBr}$ . (a) 0.12 mol %  $\text{KCN} + 0.2 \text{ mol } \% \text{ NaBr}$ . The labeled lines involve the  $\text{Na}^+$  ion and the unmarked ones are either pair modes or  $\text{Cl}^-$  perturbed modes (see Table II for the mode frequencies). (b) 0.12 mol %  $\text{KCN} + 0.02 \text{ mol } \% \text{ LiBr}$ . The labeled lines involve the  $\text{Li}^+$  ion. (c) 0.12 mol %  $\text{KCN} + 0.2 \text{ mol } \% \text{ RbBr}$ . The labeled line involves the  $\text{Rb}^+$  ion. Sample temperature is 1.7 K and the instrumental resolution  $0.04 \text{ cm}^{-1}$ .

gives an excited-state decay time of 27 msec. When the fundamental  $\text{CN}^-$  vibration of a high-concentration sample is pumped the fluorescence signature is completely different.

The emission spectrum for  $\text{KBr} + 0.12 \text{ mol } \% \text{ KCN} + 0.2 \text{ mol } \% \text{ NaBr}$  at 1.7 K is shown in Fig. 8. At this high- $\text{CN}^-$  concentration a series of sharp emission lines appear at frequencies below the pump frequency. These emission features result from the electric-dipole-mediated vibrational energy-transfer process between  $\text{CN}^-$  molecules.<sup>25</sup> This  $V$ - $V$  transfer not only leads to population of highly excited vibrational states and isotope-shifted states of the  $\text{CN}^-$  molecule, but also to population of the  $\text{CN}^-:\text{Na}^+$  complex. To conserve energy in the energy transfer from a singly excited  $\text{CN}^-$  donor ion to the  $\text{CN}^-:\text{Na}^+$  acceptor complex a lattice phonon is emitted at a frequency equal to the energy difference. This energy-transfer reaction can be written as



Since  $\Delta E$  is much larger than  $kT$  the back reaction is not allowed and vibrational energy is funneled into the  $\gamma_1$  centers. Measurement of the time-resolved fluorescence signal from the fundamental mode of the  $\gamma_1$  center and isolated  $^{13}\text{C}^{14}\text{N}^-$  centers give lifetimes of 10 and 25 msec, respectively. For the small  $^{13}\text{C}^{14}\text{N}^-$  concentration (estimated to be 0.0015 mol %),  $V$ - $V$  transfer is not important and so the measured decay time of 25 msec is the same as found for isolated  $^{12}\text{C}^{14}\text{N}^-$  molecules. The concentration of the  $\gamma_1$  centers is 0.015 mol %, a concentration where  $V$ - $V$  transfer effects have previously been observed. The shorter decay time of 10 msec found experimentally for the  $\gamma_1$  center could stem from the higher concentration; therefore, the best estimate of the excited lifetime,  $T_1$ , for the  $\gamma_1$  center is between 10–25 msec. It appears that the nearby  $\text{Na}^+$  impurity does not radically change the vibrational mode lifetime of the  $\text{CN}^-$  ion.

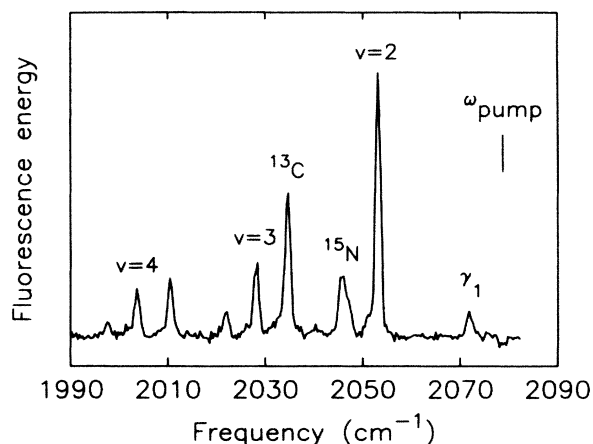


FIG. 8. Vibrational emission spectrum of  $\text{KBr} + 0.12 \text{ mol } \% \text{ KCN} + 0.2 \text{ mol } \% \text{ NaBr}$ . Sample temperature is 1.7 K and monochromator resolution is  $1.3 \text{ cm}^{-1}$ .

The measurement of  $T_1$  from the fluorescence experiment together with the saturation measurement of  $I_s$  on the 0.015 mol %  $\text{CN}^-:\text{Na}^+$  sample permit an independent estimate of  $T_2$  which can be compared with the value ( $\sim 600 \text{ MHz}$ ) obtained from a persistent hole-burning measurement. With the anharmonic  $\text{CN}^-$  oscillator approximated by two-level behavior,<sup>16</sup> then

$$T_2 = \frac{1}{4} \frac{N}{S} \frac{h\nu}{T_1 I_s}, \quad (4)$$

where  $N$  is the number density and  $S$  is the integrated absorption strength. Because of the experimental uncertainty in  $I_s$  and  $T_1$ , these values of  $T_2$  vary from 3.4 to 0.5 nsec and from

$$\Delta\nu_{\text{hole}} = \frac{2}{\pi T_2} \quad (5)$$

the calculated hole width varies from 180 to 1400 MHz in reasonable agreement with the data above.

#### IV. DYNAMICS OF PERSISTENT HOLE BURNING FOR THE $\gamma_1$ MODE

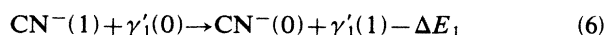
##### A. Geometry of the center

The polarization of the persistent hole-burning effect has been used to identify the orientation of the center in the crystal lattice. When a hole is burned with the laser  $E$ -field oriented along one of the [100] crystal axes then analysis with the low-power probe beam shows that no hole is produced in the polarization perpendicular to the incident burning beam polarization. In addition, if the burning beam polarization is oriented at  $45^\circ$  with respect to two [100] axes then the hole depth is independent of the probe polarization. From these experimental results it is clear that the  $\text{CN}^-$  complex cannot be oriented along the [111] crystal axes which is the equilibrium direction in the unperturbed lattice. The polarization results are consistent with the  $\text{CN}^-$  being oriented along one of the six [100] axes with the particular axis determined by the location of the near-neighbor  $\text{Na}^+$  impurity.

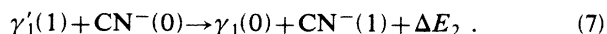
To locate the vibrational absorption of the hole-burned product state the SDL is used in conjunction with the FTIR interferometer. The diode laser is swept in frequency over the  $0.04\text{-cm}^{-1}$  wide  $\gamma_1$  line to burn away the entire absorption in one polarization since the FTIR resolution is only  $0.04 \text{ cm}^{-1}$ . After erasing the  $\gamma_1$  mode, an FTIR spectrum is obtained. Then the sample is warmed to 50 K to recover the  $\gamma_1$  mode, cooled back down to 1.7 K, and another spectrum is obtained. The experimental results are shown in Fig. 9. The top trace displays the FTIR absorption spectrum before erasing and the bottom trace shows the difference in absorption coefficient ( $\gamma_1$  erased –  $\gamma_1$  present). Figure 9 demonstrates that erasing the original  $\gamma_1$  mode centered at  $2071.83 \text{ cm}^{-1}$  produces the  $\gamma_1'$  mode at  $2077.75 \text{ cm}^{-1}$  which is almost coincident with the isolated  $\text{CN}^-$  stretch-mode frequency of  $2077.60 \text{ cm}^{-1}$ . The polarization of the  $\gamma_1$  and  $\gamma_1'$  modes are the same and the integrated absorption strength of the  $\gamma_1'$  mode is equal to  $0.9 \pm 0.2$  of the  $\gamma_1$  mode strength. This large experimental uncertainty is a consequence of the

strong absorption produced by the  $\text{CN}^-$  band in this frequency region. Note that none of the other  $\text{CN}^-$  ion-complex absorptions shown in Fig. 9 have changed so the particular  $\text{Na}^+:\text{CN}^-$  center that produces the  $\gamma_1$  line is independent from the  $\gamma_2$ ,  $\gamma_3$ , and  $\gamma_4$  absorptions. These latter spectral lines must be due to centers with distinctly different locations of the  $\text{Na}^+$  relative to the  $\text{CN}^-$  hence their numbering.

The  $\gamma_1'$  mode shows some new persistent hole-burning effects. After the  $\gamma_1'$  mode is populated as described above then a persistent spectral hole (FWHM of 100 MHz) can be burned in it with the SDL. It is also possible to sweep the SDL frequency and burn away the entire absorption line with the oscillator strength returning to the  $\gamma_1$  mode. Another interesting effect is that the entire  $\gamma_1'$  mode can be erased by tuning the diode laser anywhere in the main  $\text{CN}^-$  stretch region. Since sample heating is negligible at these low intensity levels this nonresonant erasing effect must be a consequence of the  $V$ - $V$  energy-transfer process described earlier. The reaction equations now are



and



The process is energetically possible because  $\Delta E_1 < kT$  (even at 1.7 K).

### B. Relative energies of the two configurations

The simplest hole-burning models consistent with the polarization and photoproduct data are that either the

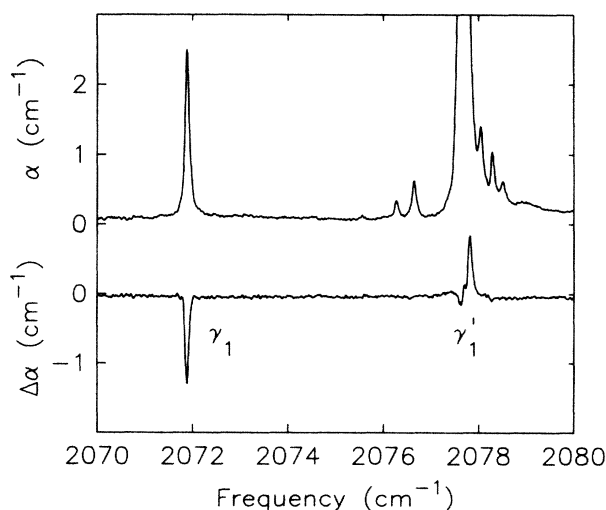


FIG. 9. Observation of the persistent hole product state. The top trace shows the FTIR absorption spectrum for the  $\text{CN}^-:\text{Na}^+$  region before hole burning on the  $\gamma_1$  mode. The lower trace shows the FTIR difference spectrum after most of the  $\gamma_1$  mode is erased with an SDL. The product state  $\gamma_1'$  has the same polarization as the hole burned in the  $\gamma_1$  mode. Sample temperature is 1.7 K and the spectral resolution is  $0.04 \text{ cm}^{-1}$ .

$\text{CN}^-$  ion remains in place and the  $\text{Na}^+$  ion moves between two positions in the lattice or that the  $\text{Na}^+$  ion remains fixed and the  $\text{CN}^-$  molecule rotates by  $180^\circ$ . The first possibility is unlikely since the stability of this hole-burning center up to almost 50 K indicates that the barrier between the two states is large whereas off-center ions in crystals usually have small barriers to movement.<sup>19</sup> For the second model, since  $\text{CN}^-$  has a large elastic dipole moment it will preferentially align in the lattice so as to minimize its elastic energy. The  $\text{CN}^-$  molecular axis points at the nearest-neighbor  $\text{Na}^+$  and the nearest-neighbor  $\text{K}^+$  ions in the plane perpendicular to the molecular axis move inward to produce the large barrier to rotation. We propose that the two required states are produced by a  $180^\circ$  rotation of the  $\text{CN}^-$  elastic dipole axis and that the inequivalence between the two states results from the interaction of the  $\text{CN}^-$  electric dipole and the  $\text{Na}^+$  impurity. In this two-state picture, which is shown in Fig. 10, only one state is populated at low temperatures and if some fraction of the centers are put in the high-energy state they remain there because of a large energy barrier which prohibits classical reorientation and makes reorientation by tunneling extremely unlikely. At high temperatures thermal activation over the barrier becomes likely, thermal equilibrium is restored and the relative population in the two configurations is governed by the Boltzmann factor.

To estimate the barrier height between configurations we use the hole refilling data which is obtained at elevated

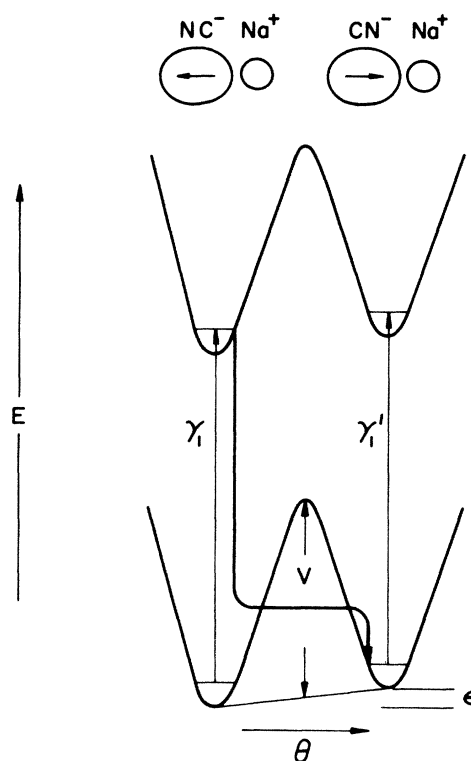


FIG. 10. Two-configuration diagram for the  $\gamma_1$  and  $\gamma_1'$  centers. The measured energies are  $\gamma_1 = 2071.83 \text{ cm}^{-1}$ ,  $\gamma_1' = 2077.75 \text{ cm}^{-1}$ ,  $V = 1040 \text{ cm}^{-1}$ , and  $\epsilon = 104 \text{ cm}^{-1}$ .



temperatures. Holes burned in the  $\gamma_1$  mode at 43 K are observed to refill with a  $1/e$  time of approximately 8 min. A classical Arrhenius relaxation rate for transitions between the two configurations

$$1/\tau = \omega_0 e^{-V/kT} \quad (8)$$

with an attempt frequency of  $\omega_0 = 1 \times 10^{13} \text{ sec}^{-1}$  gives a value for the barrier height,  $V = 1500 \text{ K}$ .

The energy mismatch between the ground-state energies of the two configurations has been obtained from high-resolution broad-band measurements of the absorption profile at elevated temperatures. By 50 K the low-temperature spectrum presented in Fig. 7 has changed dramatically into two very different kinds of spectral features which are shown in Fig. 11. The isolated  $\text{CN}^-$  ions appear to act as free rotors with characteristic  $P$  and  $R$  branches<sup>18</sup> and all of the sharp lines near the isolated  $\text{CN}^-$  stretch frequency have disappeared. However, both the  $\gamma_1$  mode and the  $^{14}\text{N}^{13}\text{C}^{16}\text{O}^-$  mode remain narrow in width, the former because it is pinned by the  $\text{Na}^+$  impurity and the latter because the long linear molecule is pinned by the lattice. It should be remembered at this point that the  $\text{NCO}^-$  mode does not fluoresce but both the sharp and broad modes associated with  $\text{CN}^-$  do. This observation demonstrates that vibrational mode lifetimes

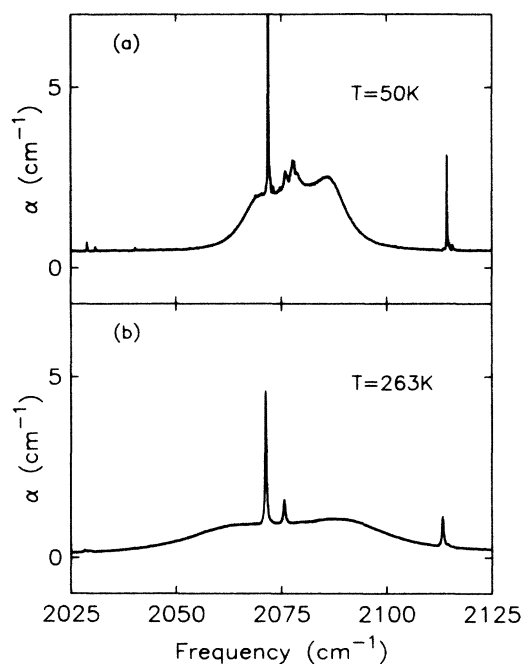


FIG. 11. Temperature dependence of the impurity-induced spectrum in the  $\text{CN}^-$  stretch-mode region. The concentrations are the same as in Fig. 8. (a) At 50 K the spectral widths of the  $\gamma_1$  mode and the  $\text{N}^{13}\text{CO}^-$  mode remain narrow while the more weakly perturbed centers  $\gamma_2$ ,  $\gamma_3$ , and  $\gamma_4$  and the isolated  $\text{CN}^-$  molecule show nearly free rotation behavior. Two of the sharp but weak lines on the left stem from the isotope shifted  $\gamma_1$  mode and the third is due to an unwanted  $\text{BO}_2^-$  impurity (see Table II for frequencies). (b) At 263 K both the  $\gamma_1$  and  $\gamma_1'$  modes can be identified. Instrumental resolution is  $0.06 \text{ cm}^{-1}$ .

cannot readily be estimated from the measured widths of spectral lines.

Another interesting result shown in Fig. 11(a) is that the  $\gamma_1'$  mode becomes observable in normal FTIR absorption spectroscopy for the first time at about 50 K (the same temperature at which  $\gamma_1$  mode holes erase rapidly). A clearer picture of both modes is obtained at even higher temperatures as shown in Fig. 11(b) with the data taken at 263 K. The sum of the strengths of the  $\gamma_1$  and  $\gamma_1'$  modes is measured to be a constant from 60 to 350 K. The temperature dependence of the ratio of the strengths is fit with a Boltzmann factor with  $\epsilon = 150 \text{ K}$  (see Fig. 10).

## V. CONCLUSIONS

If a persistent hole can be burned at low power in a vibrational mode, then a measure of the homogeneous width is obtained. The pure dephasing time of the vibrational mode  $T_2$  and lifetime in the excited vibrational state  $T_1$  are related to the effective decay time  $T_e$  measured from the homogeneous hole width by<sup>6</sup>

$$(T_e)^{-1} = (T_1)^{-1} + 2(T_2)^{-1}. \quad (9)$$

If the dephasing of the excited state is dominated by excited-state decay then  $T_2 = 2T_1$  and Eq. (9) reduces to

$$(T_e)^{-1} = 2(T_1)^{-1}. \quad (10)$$

For this limit a measurement of the homogeneous width measures  $T_1$  directly. If the excited-state decay time is unknown then a measurement of the homogeneous width still provides a lower limit for  $T_1$ , namely,

$$T_e \leq T_1/2. \quad (11)$$

For the spherical-top molecule,  $\text{ReO}_4^-$ , the excited-state decay at 1.7 K is fast enough that Eq. (10) is valid hence persistent hole widths can be directly related to the lifetime.<sup>13</sup> In the present study on  $\text{CN}^-$  complexes this is no longer the case: The hole widths are larger than found for  $\text{ReO}_4^-$  yet from the fluorescence measurement on the  $\text{CN}^-:\text{Na}^+$  mode, the  $T_1$  time is of the same order as for the isolated  $\text{CN}^-$  molecule ( $\sim 20 \text{ msec}$ ) so that Eq. (11) now applies.

Although the persistent effect can no longer by itself be used to extract information about the decay process, it still provides a high-resolution probe of the center and its environment and this probe has been used to identify and characterize a new class of ir hole-burning centers in which a  $\text{Na}^+$  or  $\text{Cl}^-$  impurity perturbs the  $\text{CN}^-$  molecule in a KBr host crystal. These low-temperature centers are listed in Table II. For temperatures above 50 K only the  $\gamma_1$  center, which corresponds to a  $\text{Na}^+$  ion in a nearest-neighbor  $\text{K}^+$  site of the  $\text{CN}^-$  molecule, is stable and produces a sharp transition even at room temperature. With increasing temperature the other centers  $\gamma_2$ ,  $\gamma_3$ ,  $\gamma_4$ ,  $\alpha_1$ , and  $\alpha_2$  break up and their sharp spectral lines disappear with the oscillator strengths transferring to the broad absorption bands identified with the free rotorlike motion<sup>18</sup> of isolated  $\text{CN}^-$ . At 1.7 K all of these centers show persistent hole burning but the most stable holes appear in the  $\gamma_1$  mode and this is the complex which has been inves-

tigated in some detail.

The combination of high-resolution FFT interferometry and polarized SDL hole burning has enabled us to identify the dynamics of this process. Since the antihole is far removed in energy from the inhomogeneous line position where the hole is burned, the second configuration ( $\gamma'_1$ ) must become populated during the vibrational deexcitation of the center in the first configuration. The transfer to the new configuration occurs about one time in one hundred thousand transition cycles.

Figure 10 shows the measured energies for the lattice-defect system approximately to scale. When the crystal is cooled slowly only the ground state of  $\gamma_1$  remains populated at 1.7 K because the energy separation between the two configurations,  $\epsilon=150$  K. Inducing the  $\gamma_1$  transition with the SDL fills the  $\gamma'_1$  ground state by cross relaxation. The crystal is no longer in thermal equilibrium since the barrier height,  $V=1500$  K, is too large for the  $\text{CN}^-$  molecule to flip by  $180^\circ$  so the complex cannot return to the  $\gamma_1$  ground state.

Once the simple geometric form of the persistent hole complex was identified, other complexes which contained  $\text{Li}^+$  or  $\text{Rb}^+$  were fabricated (see Table II) and studied but no persistent effects have been identified at 1.7 K. This null result is surprising because both an alkali and a halide impurity ion have already been used successfully as persistent complex components. The crossover must occur during vibrational deexcitation. Presumably, a transition from the excited vibrational and ground rotational state to a ground vibrational but excited rotational state in the first configuration puts the system in a region of low barrier energy so that it can tunnel to the second configuration (as shown in Fig. 10); but if so, a similar process would be expected to occur when other monovalent impurities are placed near the  $\text{CN}^-$  ion. The fact that  $\text{CN}^-$  ions in conjunction with monovalent ions in

KBr may or may not give rise to persistent effects in the vibrational spectrum suggests that the physical process behind the cross-relaxation effect is not yet clearly defined. Additional measurements on complexes containing other impurities and host lattice combinations should be made to clarify this point.

With the technique of persistent ir hole burning, isolated elastic configurations now have been identified for two different molecule-lattice combinations: the spherical-top  $\text{ReO}_4^-$  in alkali halides<sup>13</sup> and the polar diatomic  $\text{CN}^-:\text{Na}^+$  or  $\text{CN}^-:\text{Cl}^-$  in KBr. For both types the persistence occurs because of the large energy barrier which prohibits reorientation of the molecule back to the equilibrium ground-state configuration at low temperatures. No hole burning has been found for matrix isolated  $\text{NCO}^-$  or for  $\text{CN}^-$  which, perhaps, identifies two different limits for this technique: In the first case, the linear molecule is too large to undergo reorientation when excited by a vibrational quantum while in the second case, the molecule tunnels so that the thermal ground state is composed from a symmetric combination of a configuration set. Even for this latter system persistence still could occur if a large barrier existed between, say, the [100] and the [111] set of configurations but our experiments show that this is not the case for  $\text{CN}^-$ .

#### ACKNOWLEDGMENTS

Discussions with T. R. Gosnell, R. H. Silsbee, and J. P. Sethna have been particularly helpful. This work was supported in part by the U.S. Army Research Office under Grant No. DAAG-29-84-K-0206 and DAAG29-83-G-0109 and by the National Science Foundation under Grant No. DMR-85-16616. (Cornell University Materials Science Center Report No. 5798.)

<sup>1</sup>H. Dubost, L. Abouf-Marguin, and F. Legay, *Phys. Rev. Lett.* **29**, 145 (1972).

<sup>2</sup>Y. Yang and F. Lüty, *Phys. Rev. Lett.* **51**, 419 (1983).

<sup>3</sup>A. A. Gorokhovskii, R. K. Kaarli, and L. A. Rebane, *JETP Lett.* **20**, 216 (1974) [*Pis'ma Zh. Eksp. Teor. Fiz.* **20**, 474 (1974)].

<sup>4</sup>B. M. Kharlamov, R. I. Personov, and L. A. Bykovskaya, *Opt. Commun.* **12**, 191 (1974).

<sup>5</sup>L. A. Rebane, A. A. Gorokhovskii, and J. V. Kikas, *Appl. Phys. B* **29**, 235 (1982).

<sup>6</sup>J. Friedrich and D. Haarer, *Angew. Chem.* **23**, 113 (1984).

<sup>7</sup>G. J. Small, in *Spectroscopy and Excitation Dynamics of Condensed Molecular Systems*, edited by V. M. Agranovitch and R. M. Hochstrasser (North-Holland, Amsterdam, 1983), pp. 515-554.

<sup>8</sup>W. E. Moerner, *J. Mol. Electron.* **1**, 55 (1985).

<sup>9</sup>A. Winnacker, R. M. Shelby, and R. M. Macfarlane, *Opt. Lett.* **10**, 350 (1985).

<sup>10</sup>H. W. H. Lee, M. Gehrtz, E. E. Marinero, and W. E. Moerner, *Chem. Phys. Lett.* **118**, 611 (1985).

<sup>11</sup>M. Dubs and H. H. Günthard, *Chem. Phys. Lett.* **64**, 105 (1979).

<sup>12</sup>P. Felder and H. H. Günthard, *Chem. Phys.* **85**, 1 (1984).

<sup>13</sup>W. E. Moerner, A. R. Chraplyvy, A. J. Sievers, and R. H. Silsbee, *Phys. Rev. B* **28**, 7244 (1983).

<sup>14</sup>T. R. Gosnell, A. J. Sievers, and R. H. Silsbee, *Phys. Rev. Lett.* **52**, 303 (1984).

<sup>15</sup>H. Lengfellner and A. J. Sievers, *Phys. Rev. B* **31**, 2591 (1985).

<sup>16</sup>W. E. Moerner, A. R. Chraplyvy, and A. J. Sievers, *Phys. Rev. B* **29**, 6694 (1984).

<sup>17</sup>A preliminary report already has been published: R. C. Spitzer, W. P. Ambrose, and A. J. Sievers, *Opt. Lett.* **11**, 428 (1986).

<sup>18</sup>W. D. Seward and V. Narayanamurti, *Phys. Rev. B* **148**, 463 (1966).

<sup>19</sup>V. Narayanamurti and R. O. Pohl, *Rev. Mod. Phys.* **42**, 201 (1970).

<sup>20</sup>F. Lüty, *Phys. Rev. B* **10**, 3677 (1974).

<sup>21</sup>H. U. Beyeler, *Phys. Rev. B* **11**, 3078 (1975).

<sup>22</sup>H. de Vries and D. A. Wiersma, *J. Chem. Phys.* **72**, 1851 (1980).

<sup>23</sup>L. H. Greene and A. J. Sievers, *Phys. Rev. B* **31**, 3948 (1985).

<sup>24</sup>K. P. Koch, Y. Yang, and F. Lüty, *Phys. Rev. B* **29**, 5840 (1984).

- <sup>25</sup>R. W. Tkach, T. R. Gosnell, and A. J. Sievers, *Opt. Lett.* **9**, 122 (1984).
- <sup>26</sup>T. R. Gosnell, R. W. Tkach, and A. J. Sievers, *J. Lumin.* **31-32**, 166 (1984).

- <sup>27</sup>T. R. Gosnell, R. W. Tkach, and A. J. Sievers, *Infrared Phys.* **25**, 35 (1985).
- <sup>28</sup>T. R. Gosnell, A. J. Sievers, and C. R. Pollock, *Opt. Lett.* **10**, 125 (1985).